COMPARATIVE FATIGUE ANALYSIS OF OFFSHORE STRUCTURES USING SPECTRAL AND DETERMINISTIC METHODS

*Lurohman Mamin Masturi¹, Alvin Reynaldi¹, Farid Putra Bakti¹, Ricky Lukman Tawekal¹

¹Faculty of Civil and Environmental Engineering, Institut Teknologi Bandung, Indonesia

*Corresponding Author, Received: 06 Nov. 2024, Revised: 08 May 2025, Accepted: 11 May 2025

ABSTRACT: The jacket of bottom fixed type offshore structures has to be designed its tubular connections to sustain the cyclic loading induced by the ocean waves throughout their operation life. In this study, two primary methods for assessing fatigue life are applied to evaluate three different structures characterized by their distinct natural periods. These structural models that varied in mass and stiffness are prepared for sensitivity study to evaluate consistency in the results with respect to the effect of structure configurations on fatigue life using deterministic fatigue and spectral fatigue. The deterministic method solely relies on linear wave theory in the selection of wave parameters, while the spectral method accounts for the structural responds to determine wave parameters. In this study, the wave probability distribution is tabulated using a single wave scatter data (presented in H_s and T_p), in which the Longuet-Higgins' method is applied to obtain the individual wave distribution (presented in H and T) to be used in the deterministic fatigue analysis. In addition, this study also evaluates the application of Longuet-Higgins' wave conversion theory for three structural models with varying natural periods $(T_n = 1.6 \text{ s}, 3.1 \text{ s}, \text{ and } 4.6 \text{ s})$. In order to minimize the discrepancies between deterministic fatigue and spectral fatigue, the structural normalized stresses are calculated dynamically to obtain the dynamic response, and identical fatigue parameters were applied: the API X' S-N curve and Efthymiou's stress concentration factor (SCF) theory. The results show the deterministic fatigue has comparable patterns to spectral fatigue as it shows consistent patterns. This study concludes that dynamic analysis is crucial for assessing fatigue life and highlights the importance of selecting appropriate wave height (H) and period (T) ranges for Longuet-Higgins' wave conversion.

Keywords: Longuet-Higgins' Wave Conversion Theory, Deterministic Fatigue, Spectral Fatigue

1. INTRODUCTION

Fixed jacket platforms are widely used in offshore oil and gas exploration. These structures typically consist of prefabricated steel tubular frames, which offer an optimal balance of low drag coefficient, high buoyancy, and a high strength-to-weight ratio [1]. Their simplicity, reliability, cost-effectiveness, and rapid construction make them a preferred choice for engineers [2]. However, in the oil and gas industry, jacket platforms face significant challenges, particularly regarding fatigue loads on welded joints. The uncertainty in hot-spot stress at these joints is significantly higher, making fatigue damage a critical design factor and requiring accurate fatigue assessment [3-5].

In offshore structures, fatigue damage is primarily caused by cyclical wave loading. Fatigue damage estimation can be approached through two primary methods: the fracture mechanics approach and the S-N curve approach. The S-N curve approach, which is more commonly used, includes three methods: simplified fatigue analysis, deterministic fatigue analysis, and spectral fatigue analysis [6].

Comparative study on various fatigue analysis methods has been conducted by Sulaksono [6] and Rohith [7]. These studies compared the deterministic and spectral fatigue analysis for various types of welded joint type and bracing type. Both studies show

that deterministic fatigue analysis typically gives more conservative results compared to the fatigue analysis, regardless of the joint type and bracing type. Sulaksono [6] further shows that even though the resulting fatigue life is different, both deterministic and spectral fatigue analysis shows the same fatigue damage distribution as function of its elevation. However, Sulaksono [6] and Rohith [7] leave several gaps in their study. Both studies stated the possibility of the structural natural period affecting the outcome of the result, a factor which was rarely examined in similar studies. Furthermore, both studies failed to clearly explain or prove that the results are not affected by their choice of the individual wave and irregular wave scatter diagram.

In any fatigue analysis methods, one of the primary input is wave data. The wave parameters are often represented using irregular wave scatter data, which statistically describes significant wave height (H_s) and peak wave period (T_p) . Alternatively, individual wave probability of occurrence can also describe sea states, using individual wave height (H) and individual wave period (T). It is well known that deterministic fatigue analysis is sensitive to the choice of the individual (regular) wave height, wave period, and their corresponding probability of occurrence (Rohith [7]), further emphasizing the need of a proper conversion method between the random waves and individual waves sea state..

analysis Two fatigue methods, namely deterministic fatigue and spectral fatigue, are evaluated in this study. Deterministic fatigue analysis will be performed using individual wave probability of occurrence data, while spectral fatigue analysis will utilize irregular wave scatter data. Both analyses are performed based on the same set of irregular wave data, which is then converted to the individual wave data using Longuet-Higgins' conversion theory, ensuring the preservation and consistency of the probability distribution between the two. The impact of natural period to the comparative result is also examined by varying the weight density, while keeping the rest of structural configuration as similar as possible.

2. RESEARCH SIGNIFICANCE

The significance of the present study is highlighted by the use of Longuet-Higgins' joint probability theory, which may serve as an example of how to properly convert the irregular scatter diagram to individual wave scatter diagram when conducting deterministic fatigue analysis in the case limited data provided. Furthermore, sensitivity analysis of how the structural natural period affects both the fatigue life and fatigue damage distribution on both methods may prove useful when defining which method is more suitable to be used on each unique case that one might find in the real world application.

3. LONGUET-HIGGINS' JOINT PROBABILITY THEORY

The Longuet-Higgins' distribution is a theoretical joint probability density function for wave periods and amplitudes of sea waves [8]. This joint distribution provides an alternative theoretical approach, based on narrowband theory to convert irregular wave data probability into individual wave probability. The joint probability of individual wave data is formulated as Eq. (1).

$$p(R,S,Z) = L(v) \exp \left[-R^2 \left(1 + \frac{\left(1 - \frac{1}{S} \right)^2}{v^2} \right) \right] \frac{2R^2}{S^2 v \sqrt{\pi}}$$
 (1)

$$L(v) = \frac{2}{1 + \frac{1}{\sqrt{1 + v^2}}} \tag{2}$$

$$R = \frac{H}{H_{rms}} \tag{3}$$

$$S = \frac{T}{T_m} \tag{4}$$

$$T_m = \frac{m_0}{m_1} \tag{5}$$

$$v = \sqrt{\frac{T_m^2}{T_z^2} - 1} \tag{6}$$

$$T_Z = \sqrt{\frac{m_0}{m_2}} \tag{7}$$

where m_n denotes the n^{th} order moment of the wave spectrum, T_m is the mean period, T_z is the mean zero-up crossing period, v is the spectral width of the spectrum, L(v) is a normalization factor, R and T denote dimensionless wave height and period respectively.

Irregular wave scatter data in Table 1 is converted using Longuet-Higgins' wave conversion theory to obtain individual wave probability of occurrence which shown in Table 2. The H and T ranges for Longuet-Higgins' wave conversion are selected to match the irregular wave scatter data, ensuring comparability. After conversion, the wave period shifts from $T_p = 5.5$ s (see Table 1) to T = 3.5 s (see Table 3). This period shift is validated in Section 2.1.

3.1 Period Shifting Validation

To validate the period shift, a wave dataset (H_s = 0.75 m, Tp = 5.5 s) is selected to generate the JONSWAP wave spectrum, as shown in Fig. 2. From this spectrum, the crossing period is determined using the spectral moment (see Eq. (7)) and time series analysis. The time series (see Fig. 1) is generated through the inverse fast Fourier transform (IFFT).

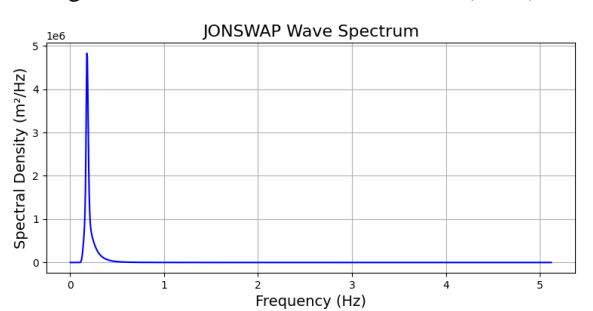


Fig. 1 JONSWAP Spectrum

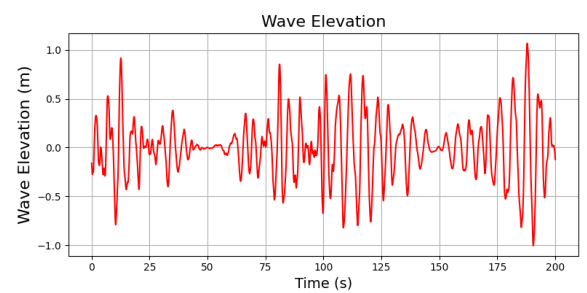


Fig. 2 Time series

From the JONSWAP spectrum, the zero-crossing period is calculated as 4.43 s, while the time series analysis resulting a zero-crossing period of 4.51 s. This confirms a shift from the spectral wave period (T_p) to the individual wave period (T). Goda [9], in his book shows the ratio between individual wave period (T) and peak period (T_p) for JONSWAP gamma factor 3.3 is 0.80. Which indicates there is a period shifting from (T_p) to T and (T_p) must be greater than T. This experiment validates the period shifting following Longuet-Higgins' wave

conversion.

Table 1. Irregular Wave Scatter Data

Significant Wave					I	Peak Perio	d, Tp (sec	:)					- Total
Height, Hs (m)	3.5	4.5	5.5	6.5	7.5	8.5	9.5	10.5	11.5	12.5	13.5	14.5	Total
0.25	0.009	0.032	0.016	0.001	0.002	0.001	0.001	0.001	0.000	0.000	0.000		0.064
0.75	0.023	0.120	0.139	0.071	0.032	0.029	0.017	0.009	0.006	0.003	0.001		0.447
1.25		0.018	0.068	0.041	0.053	0.021	0.016	0.012	0.007	0.003	0.001	0.001	0.241
1.75			0.007	0.023	0.040	0.032	0.007	0.004	0.003	0.002	0.001	0.001	0.120
2.25				0.003	0.019	0.029	0.009	0.002	0.001	0.001			0.063
2.75					0.003	0.022	0.010	0.001					0.036
3.25						0.006	0.008	0.001					0.015
3.75						0.001	0.005	0.001					0.006
4.25							0.002	0.002					0.004
4.75								0.001					0.001
Total	0.032	0.17	0.23	0.139	0.149	0.141	0.073	0.032	0.018	0.009	0.003	0.002	1.000

Table 2. Individual Wave Number of Occurrences

II (m)		Period, T (s)										
H (m)	3.5	4.5	5.5	6.5	7.5	8.5	9.5	10.5	11.5	12.5	13.5	14.5
0.25	1671852	416825	226166	128439	76621	47889	31280	21272	14993	10903	8145	6229
0.75	963593	522549	305695	172871	98799	57589	34483	21350	13722	9159	6335	4525
1.25	185027	202096	149520	92650	53993	30999	17919	10577	6441	4070		
1.75	32592	74267	75917	52039	30100	16603	9138	5120				
2.25	4846	24289	36752	28946	16821	8872	4625					
2.75		7323	16985	15843	9490	4836						
3.25			7406	8413	5317							
3.75				4324								

Table 3 Individual Wave Probability

II (m)						Period	, T (s)						
H (m)	3.5	4.5	5.5	6.5	7.5	8.5	9.5	10.5	11.5	12.5	13.5	14.5	Total
0.25	0.271	0.068	0.037	0.021	0.012	0.008	0.005	0.003	0.002	0.002	0.001	0.001	0.431
0.75	0.156	0.085	0.050	0.028	0.016	0.009	0.006	0.003	0.002	0.001	0.001	0.001	0.358
1.25	0.030	0.033	0.024	0.015	0.009	0.005	0.003	0.002	0.001	0.001			0.122
1.75	0.005	0.012	0.012	0.008	0.005	0.003	0.001	0.001					0.048
2.25	0.001	0.004	0.006	0.005	0.003	0.001	0.001						0.020
2.75		0.001	0.003	0.003	0.002	0.001							0.009
3.25			0.001	0.001	0.001								0.003
3.75				0.001									0.001
Total	0.463	0.202	0.133	0.082	0.047	0.027	0.016	0.009	0.006	0.004	0.002	0.002	0.993

3.2 Total Duration Verification

Irregular wave scatter data is for one year, to ensure the Longuet-Higgins' wave conversion is conserved, the total duration of the conversion results must be validated. The irregular wave data is recorder for each hour. Therefore, the number of occurrences of irregular wave scatter data in Table 1 can be calculated by this following formula,

$$n_i = p_i * 365 \frac{day}{year} * 24 \frac{hours}{day} * 60 \frac{min.}{hours} * 60 \frac{sec.}{min} \tag{8}$$

Where p_i is the probability of each pair of H_s and T_p . Total duration of irregular wave scatter data is 31,422,470 seconds while the total duration of individual wave in Table 2 is 29,563,787 seconds. Since it shows 6% differences, which falls within the

acceptable range of -10% to +15% as indicated by NDBC [10]. Therefore, the individual wave data derived from Longuet-Higgins' wave conversion is considered valid.

4. FATIGUE ANALYSIS

4.1 Structural Model

Structures with three different fundamental natural periods are modeled. Three modeled structures are simple X-braced with four leg fixed jackets with a water depth of 50 meters. The natural period for each structure is varied by altering the weight density while keeping the rest of structural characteristics the same. Fig. 3 presents the identical model for all structures while the properties of each structure are presented in Table 4.

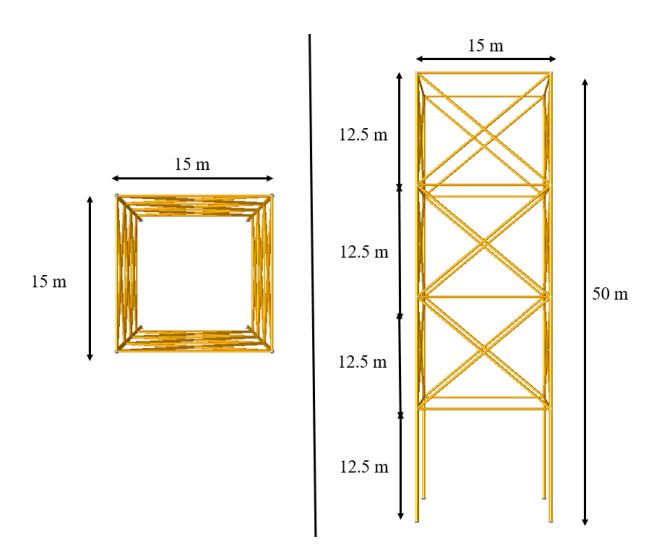


Fig. 3 Structural Model

The variation of weight density has a minor effect on the CoG location of the jacket structure model, hence the load distribution on the jacket can be assumed to be unchanged for three structural models. Since the same jacket configuration and tubular joint profiles are applied, the similar Stress Concentration Factors (SCF) of simply tubular joints are identified. Therefore, stress distribution will be proportional for three jacket models.

In the oil and gas industry, the offshore platforms has been conservatively designed to represent the platform condition at the end of the platform design life. The design assumption can differ in each platform depending on the environmental condition, jacket configuration, design purposes, and the company safety standard. Therefore, several assumptions have been made to narrow the study area, at which the paper contribution can be converged and defined in the introduction section. In this paper, the dissipation damping of 2% is proposed for fatigue

analysis in accordance with the common design practice recommended by API RP 2A [11]. A conservative assumption is made in this study regarding the overall structure capacity. The structure was modeled based on the cross-section that has been reduced due to corrosion as an effect of direct exposure to the harsh environmental condition. In the application, the tubular wall thickness is reduced by 6 inches from the outside diameter for the structural members in the splash zone elevation. By this means, the effect of corrosion in time scale is out of paper focus discussion.

Table 4. Structural Properties

	Structura	** **		
Properties	Tn < 3 seconds	Tn ~ 3 seconds	Tn > 3 seconds	Unit
Natural Period	1.60	3.10	4.60	S
Yield Stress (f_y)	345	345	345	MPa
Weight Density	0.79	18.84	49.46	ton /m³
Leg (OD X WT)*	40 X 3.5	40 X 3.5	40 X 3.5	cm
Hor. Bracing (OD X WT)*	25 X 2.0	25 X 2.0	25 X 2.0	cm
X-Bracing (OD/WT)*	25/3.5	25/3.5	25/3.5	cm
Joint Load	1167.4	1167.4	1167.4	kN

^{*)} wall thickness is reduced at the splash zone elevation

4.2 Dynamic Analysis

To maintain consistency on the dynamic effects of the jacket for both fatigue analysis, the same dynamic parameters are implemented during the dynamic analysis stage prior to proceeding with the comparison study of deterministic and spectral fatigue analysis. For dynamic analysis, the force is calculated dynamically using the dynamic equation which formulated as in Eq. (10).

$$[M][\ddot{U}] + [C][\dot{U}] + [K][U] = [F] \tag{9}$$

$$[f] = [k][u] \tag{10}$$

where M is the generalized mass matrix, C is the generalized damping matrix, K is the generalized stiffness matrix, U is the dynamic displacement, \dot{U} is the velocity, \ddot{U} is the acceleration, F is the force acting on the structure, f is the dynamic force, k is the element stiffness, and u is the dynamic displacement, which is obtained from Eq. (9).

In the numerical modeling, modal analysis is

employed to transform the equation of motion (see Eq. (9)) into a series of uncoupled equation (see Eq. (11)). The key idea is to express the dynamic displacement u as a sum of mode shapes by modal coordinates, which can be expressed as,

$$u = \sum_{i=1}^{n} \Phi_i \, q_i \tag{11}$$

Where Φ_i is the mode shapes (eigenvector) and q_i is the modal coordinate. Employing this modal coordinate, Eq. (9) can be expressed as,

$$[m_i][\ddot{q_i}] + [c_i][\dot{q_i}] + [k_i][q_i] = [f_i]$$
(12)

$$m_i = \Phi_i^T M \Phi_i \tag{13}$$

$$c_i = \Phi_i^T C \Phi_i \tag{14}$$

$$k_i = \Phi_i^T K \Phi_i \tag{15}$$

$$f_i = \Phi_i^T F \Phi_i \tag{16}$$

Where m_i is the mode mass, c_i is modal damping k_i is modal stiffness, and f_i is modal force.

The amount of mode shape considered in dynamic analysis ensures the participation of masses. In this study, 20 mode shapes are utilized. According to design practice, the minimum mass participation shall be 90% in all directions. The dynamic analysis on the jacket structural model shows that the first mode shape has structural period of 1.6 s, 3.1 s, and 4.6 s for three studied models, respectively.

4.3 Deterministic Fatigue Analysis

Deterministic fatigue analysis employed individual wave data (*H* and *T*) derived from the same irregular wave scatter data using Longuet-Higgins' joint probability conversion theory. API X' S-N curve is utilized and Efthymiou SCF theory with minimum value of 1.5 is selected [11].

For each wave (H and T), the stress range ($\Delta\sigma_{HSSR}$) is calculated as the difference between the maximum and minimum dynamic stress. At joint locations, the stress concentration factor (SCF) is applied to account for local stress amplification, which can be expressed as in Eq. (17).

$$\Delta \sigma_{HSSR} = SCF \times \Delta \sigma_n \tag{17}$$

Where $\Delta \sigma_{HSSR}$ is the hot spot stress range, $\Delta \sigma n$ is the nominal stress. Cumulative fatigue damage is calculated using Palmgren-miner's rule which is formulated as in Eq. (18).

$$D = \sum_{i=1}^{n} \frac{n_i}{N_i} \tag{18}$$

Where n_i is the number of cyclic loads (obtained

from Longuet-Higgins' wave conversion theory) and N_i is the number of cycles to failure, which is determined by the API X' S-N curve

4.4 Spectral Fatigue Analysis

An alternative for analyzing fatigue life is spectral fatigue analysis [12]. Spectral fatigue analysis has gained reliability in estimating fatigue damage for offshore structures due to its accurate assessment of stress response and fatigue damage [13-15]. Spectral fatigue analysis calculates the fatigue damage based on the power spectral density (PSD) of stress, which is derived from the PSD of random loads [13], which means it considers the distribution of energy over the entire wave frequency ranges. The relationship between a given sea state and the stress spectrum [14] can be expressed as in Eq. (19).

$$S_{\sigma\sigma-nominal}(\omega) = |H(\omega)|^2 S_{\eta\eta}(\omega)$$
 (19)

Where $S_{\sigma\sigma-nominal}(\omega)$ is the nominal stress spectrum, $S_{\eta\eta}(\omega)$ is the wave spectrum, and $|H(\omega)|$ is the transfer function from wave spectrum to stress spectrum, the JONSWAP spectrum is utilized. Since the spectral fatigue analysis utilizing stress spectrum. This wave data is omnidirectional and analyzed for 8 directions and the JONSWAP spectrum [15] is utilized which is formulated as in Eq. (20).

$$S_{(\omega)} = \frac{\alpha g^2}{\omega^5} exp \left[-\frac{5}{4} \left(\frac{\omega_p}{\omega} \right)^4 \right] \gamma^r \tag{20}$$

$$r = exp\left[-\frac{(\omega - \omega_p^2)}{2\sigma^2 \omega_n^2}\right] \tag{21}$$

$$\gamma = \begin{cases} 5.0 & \phi \le 3.6 & \phi = \frac{T_p}{\sqrt{H_s}} \\ \exp(5.75 - 1.15\phi) & 3.6 < \phi < 5.0 & \phi = \frac{T_p}{\sqrt{H_s}} \\ 1.0 & \phi \ge 5.0 & \phi = \frac{T_p}{\sqrt{H_s}} \end{cases}$$
(22)

$$\sigma = \begin{cases} 0.07, & \text{if } \omega \le \omega_p \\ 0.09, & \text{else} \end{cases}$$
 (23)

Where $\alpha = 8.1 \times 10^{-3}$ is a Phillips constant, g is the acceleration due to gravity, Hs is the significant wave height in meters, and T_p is the spectral peak period in seconds.

Transfer function is typical for each structure and it is derived from dynamic equation of motion in Eq. (9). Since the spectral fatigue analysis utilizing stress spectrum, the hot spot stress is calculated by Eq. (24).

$$S_{\sigma\sigma-HSS}(\omega) = SCF^2 \times S_{\sigma\sigma-nominal}(\omega)$$
 (24)

Where $S_{\sigma\sigma-HSS}(\omega)$ is the local hot spot stress spectrum and $S_{\sigma\sigma-nominal}(\omega)$ is the nominal stress spectrum. Efthymiou SCF theory with minimum

value of 1.5 is selected [11]. The damage is calculated using spectral moment, which is calculated as follows,

$$\sigma_{rms}^2 = m_0 = \int_0^\infty S_{\sigma\sigma-HSS}(\omega)d\omega$$
 (25)

$$T_z = \sqrt{\frac{m_0}{m_2}} = \sqrt{\frac{\int_0^\infty S_{\sigma\sigma - HSS}(\omega)d\omega}{\int_0^\infty \omega^2 S_{\sigma\sigma - HSS}(\omega)d\omega}}$$
 (26)

$$p(S) = \frac{S}{\sigma_{\text{rms}}^2} \exp\left(-\frac{S^2}{2\sigma_{\text{rms}}^2}\right)$$
 (27)

$$N = \frac{mL}{T_Z} \tag{28}$$

$$dD = \frac{N}{N_F(s)}p(s) ds \tag{29}$$

$$D = \frac{N}{\sigma_{\rm rms}^2} \int_0^\infty \frac{S}{\sigma_{\rm rms}^2} \exp\left(-\frac{S^2}{2\sigma_{\rm rms}^2}\right) ds \tag{30}$$

Where σ_{rms}^2 is the root mean square related to zeroth spectral moment (m_0) of stress spectrum, $H(\omega)$ is the stress transfer function, $S_{\sigma\sigma-HSS}(\omega)$ is the stress spectrum, T_Z is the zero crossing period, p(S) is the narrow-band stress range distributionn, S is the stress range, N is number of cycles, L is the design life of the structure, m is the probability from irregular wave scatter data, $N_F(s)$ is the number of cycles to failure, and D is the damage.

5. RESULTS AND ANALYSIS

The results of this study include the fatigue life for deterministic fatigue analysis and spectral fatigue analysis.

5.1 Fatigue Life for Each Structure

The fatigue life of three structural model with natural periods $T_n=1.6\,\mathrm{s}$, $3.1\,\mathrm{s}$, and $4.6\,\mathrm{s}$ was evaluated using spectral fatigue and deterministic fatigue methodologies. Spectral fatigue analysis resulting higher fatigue life. In contrast, deterministic method which employing Longuet-Higgins' individual wave data resulting lower fatigue life. This difference is due to the higher wave loads of linear sinusoidal waves compared to the irregular waves that comprise the summation of the regular wave with different wave height, wave period, and wave phase.

Across elevations, the fatigue life varies significantly. For the topmost joints (Joint ID 1000 series), the low fatigue life at the elevation (-) 12.5 m - (-) 25.0 m is primarily due to the central of damage for wave loads located nearly on that jacket elevation. In contrast, joints in the 2000 and 3000 series exhibit increasing fatigue life with depth, as wave particle motion decreases at greater depths. However, the bottommost joints (4000 series) experience reduced fatigue life due to the higher bending stress occured

closed to the fixity point.

The up-and-down fatigue life pattern for all elevations is consistent between deterministic fatigue and spectral fatigue for each structure that can be seen in Table 5 until Table 7. The joint location based on their ID can be found in Fig. 4.

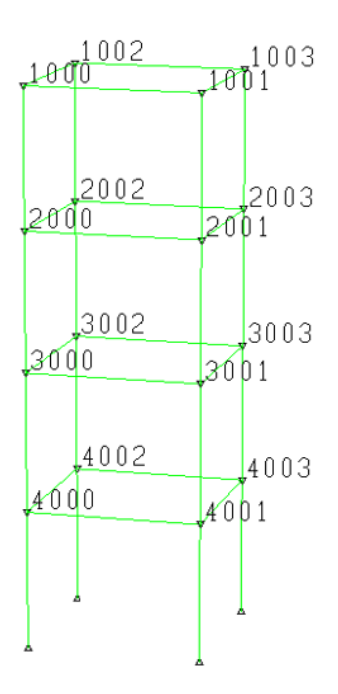


Fig. 4 Joint ID

Table 5. Comparative Fatigue Life for Structure with $T_n = 1.6$ seconds

ELEVATIONS	IODIE ID	FATIGUE LIFE (YEARS)			
(m)	JOINT ID	DET	SPEC		
	1000	26	24		
0.00	1001	26	24		
0.00	1002	26	24		
	1003	26	24		
	2000	332	5785		
12.5	2001	330	5760		
-12.5	2002	330	5760		
	2003	335	5975		
	3000	5405	40070		
25.0	3001	4357	41282		
-25.0	3002	4357	41258		
	3003	5351	40148		
	4000	335	588		
27.5	4001	335	588		
-37.5	4002	335	587		
	4003	335	588		

Table 6. Comparative Fatigue Life for Structure with $T_n = 3.1$ seconds

ELEVATIONS	IODITE ID	FATIGUE LIFE (YEARS)			
(m)	JOINT ID	DET	SPEC		
	1000	23	26		
0.00	1001	23	26		
0.00	1002	23	26		
	1003	23	27		
	2000	231	2824		
12.5	2001	232	2831		
-12.5	2002	232	2832		
	2003	221	2859		
	3000	179	469		
25.0	3001	179	469		
-25.0	3002	179	468		
	3003	179	469		
	4000	12	80		
27.5	4001	12	80		
-37.5	4002	12	80		
	4003	12	80		

Table 7. Comparative Fatigue Life for Structure with $T_n = 4.6$ seconds

ELEVATIONS	IONE ID	FATIGUE LIFE (YEARS)			
(m)	JOINT ID	DET	SPEC		
	1000	19	24		
0.00	1001	19	24		
0.00	1002	19	24		
	1003	19	24		
	2000	55	1305		
10.5	2001	55	1299		
-12.5	2002	55	1298		
	2003	55	1321		
	3000	10	448		
25.0	3001	10	433		
-25.0	3002	10	432		
	3003	10	438		
	4000	4	52		
27.5	4001	4	52		
-37.5	4002	4	52		
	4003	4	52		

5.2 Fatigue Life Across Structure

The patterns in Table 8 and Table 9 are consistent, as the natural period of the structure increases, the fatigue life decreases across structural models. This trend is primarily driven by near resonance effect.

When the natural period approaches the dominant wave period, resonance occurs, leading to higher dynamic amplification factors. Resonance amplifies the stress ranges, accelerating fatigue damage and resulting lower fatigue life. For example, structure with $T_n = 1.6$ s, shows the highest fatigue life among all structural models, due to T_n being far from dominant wave periods (T = 3.5 s).

Structure with $T_n=3.1$ s might be expected to exhibit the lowest fatigue life due to resonance effect. However, the results show that the fatigue life is higher than structue with $T_n=4.6$ s. This is primarily due to the lower amplification of structural response compared with $T_n=4.6$ s. In addition, waves at $T_p=3.5$ s have lower wave heights compared to those at $T_p=4.5$ s, leading to less fatigue damage.

Structure with $T_n=4.6$ s resulting in the lowest fatigue life due to near resonance with higher wave probability that occurred at range $T_p=4.5-5.5$ s. This alignment between $T_n=4.6$ s and $T_p=4.5$ s led to significant dynamic amplification of structural responses, resulting in higher stress ranges and lower fatigue life due to the higher probability of resonance occurred.

Table 8. Deterministic Fatigue Across All Structures Comparison

TOTALE -	DETERMINISTIC FATIGUE LIFE (YEARS)						
JOINT -	$T_n \ 1.6 \ s$	$T_n \ 3.1 \ s$	$T_n = 4.6 \text{ s}$				
1000	26	23	19				
1001	26	23	19				
1002	26	23	19				
1003	26	23	19				
2000	332	231	55				
2001	330	232	55				
2002	330	232	55				
2003	335	221	55				
3000	5405	179	10				
3001	4357	179	10				
3002	4357	179	10				
3003	5351	179	10				
4000	335	12	4				
4001	335	12	4				
4002	335	12	4				
4003	335	12	4				

Table 9. Spectral Fatigue Across All Structures Comparison

LODE	SPECTRAL FATIGUE LIFE (YEARS)						
JOINT -	$T_n 1.6 \text{ s}$	$T_n \ 3.1 \ s$	<i>T_n</i> 4.6 s				
1000	24	26	24				
1001	24	26	24				
1002	24	26	24				
1003	24	27	24				
2000	5785	2824	1305				
2001	5760	2831	1299				

Table 9. Spectral Fatigue Across All Structures Comparison (Continued)

	SPECTRAL FATIGUE LIFE (YEARS)						
JOINT -	<i>T_n</i> 1.6 s	<i>T_n</i> 3.1 s	$T_n = 4.6 \text{ s}$				
2002	5760	2832	1298				
2003	5975	2859	1321				
3000	40070	469	448				
3001	41282	469	433				
3002	41258	468	432				
3003	40148	469	438				
4000	588	80	52				
4001	588	80	52				
4002	587	80	52				
4003	588	80	52				

6. CONCLUSION

This study demonstrates that in general, the spectral fatigue method resulting in the fatigue life predictions around 10 times higher compared to deterministic fatigue analysis in the jacket elevation around the wave central damage. In the other elevations, the fatigue results are comparable across all structure models. This emphasizing implementation of wave loads originates from wave spectrum in the fatigue assessment. The wave loads of the spectral approach accounts for the statistical distribution of wave energy across all frequencies, providing a more comprehensive representation of sea state variability. In contrast, deterministic methods, which rely on individual wave height (H) and period (T) pairs, may underestimate fatigue life due to their inability to capture the full range of waveinduced loading scenarios. This result supports the finding that presented in Sulaksono [6] and Rohith [7].

The study results observe similar patterns of the fatigue damage in every level of jacket bracing for all structures. By solving the dynamic equation of motion, this study provides realistic fatigue life predictions that account for transient loading and structural dynamics. A key finding is the shift in the scatter diagram when converting irregular wave scatter data $(H_s \text{ and } T_p)$ to individual wave data $(H_s \text{ and } T_p)$ and T) using Longuet-Higgins' joint probability conversion theory. This shift arises because the conversion process redistributes wave energy across height-period pairs, altering the statistical representation of the sea state. While this shift does not significantly affect the overall fatigue life trends, it highlights the importance of selecting appropriate wave height and period ranges for analysis. Properly defining these ranges minimizes the impact of energy redistribution and ensures accurate fatigue life predictions.

The study also reveals that structures with higher natural periods (T_n) indicating higher flexibility, are

more prone to fatigue damage, as evidenced by the consistent reduction in fatigue life across all methodologies. This trend highlights the importance of dynamic stress analysis in capturing resonance effects, which amplify structural responses when wave periods approach the structure's natural periods.

In general, the deterministic fatigue analysis gives a more conservative results. However, note that the smallest fatigue life occurs on the same joint and the same pattern across all cases, in both the spectral and deterministic analysis. Thus, we can concur that as long as the individual wave scatter distribution is accounted properly, the deterministic approach may still give a useful fatigue analysis result.

7. ACKNOWLEDGMENTS

The research for this paper is funded by a grant from Faculty of Civil and Environmental Engineering, Institut Teknologi Bandung, through 2024 Research and Community Service Program (P2MI) for Offshore Engineering Research Group. The authors gratefully acknowledge this support.

8. NOMENCLATURE

- [C] = Generalized damping matrix

- c_i = Modal damping at i mode

- D = Damage

- f_i = Modal force at i mode

g = Gravity acceleration

- H = Individual wave height

- H_s = Significant wave height

- $|H(\omega)|$ = Transfer function wave to stress

- [K] = Generalized stiffness matrix

- k_i = Modal stiffness at i mode

- L = Design life of the structure

- L(v) = Normalization factor

- [M] = Generalized mass matrix

- m_i = Mode mass at i

- $m_n = n^{th}$ order moment of the wave spectrum

- N = Number of cycles

- $N_F(s)$ = Number of cycles of failure

- p(S) = Narrow-band stress range distribution

- p_i = Join probability each pair of H_s and T_p

- q_i = Modal coordinate at i mode

- R = Dimensionless wave height

- S = Stress range

- SCF = Stress concentration factor

- $S_{\sigma\sigma-nom}$ = Nominal stress spectrum

- $S_{\eta\eta}(\omega)$ = Wave spectrum

- T = Dimensionless wave period

- T = Individual wave period

- T_m = Mean zero period

- T_n = Structure natural period

- T_p = Peak wave period

- \vec{U} = Displacement

- \dot{U} = Velocity

- \ddot{U} = Acceleration
- v = Spectral width
- ζ = Damping ratio
- σ_{rms}^2 = Spectrum area
- $\Delta \sigma_{HSSR}$ = Stress range
- $\Delta \sigma_n$ = Nominal stress
- Φ_i = Mode shape (eigenvector) at i

9. REFERENCES

- [1] Jia, J. "An efficient nonlinear dynamic approach for calculating wave induced fatigue damage of offshore structures and its industrial applications for lifetime extension," Applied Ocean Research, 2008. https://doi.org/10.1016/j.apor.2008.09.003
- [2] Yang, Y., Ying, X., Guo, B. and He, Z., "Collapse safety reserve of jacket offshore platforms subjected to rare intense earthquakes,"

 Ocean Engineering, 2017.

 https://doi.org/10.1016/j.oceaneng.2016.12.010
- [3] Oyegbile, A. D. and Muskulus, M. "Enhancing fatigue reliability prediction of offshore wind turbine jacket joints through individual uncertainties for each degree of freedom of stress concentration factor," Marine Structures, 2024.https://doi.org/10.1016/j.marstruc.2024.10 3634
- [4] Song, X. and Wang, S. "A novel spectral moments equivalence based lumping block method for efficient estimation of offshore structural fatigue damage," International Journal of Fatigue, 2019. https://doi.org/10.1016/j.ijfatigue.2018.09.016
- [5] Tawekal, R. and Iqbal, M. "Fatigue reliability index of jacket offshore platform based on fracture mechanics," in EASEC-11 Eleventh East Asia-Pacific Conference on Structural Engineering and Construction, 2008.
- [6] Sulaksono, T., Ananto, A. S. and Artanti, L. D. "Comparative analysis of spectral and deterministic methods for estimating fatigue life in joint of fixed jacket platform in the Andaman Sea Myanmar," in E3S Web of Conference, 2024.https://doi.org/10.1051/e3sconf/20244790 7018
- [7] Retnamma, J. "Deterministic and spectral fatigue analysis of tubular joints of a jacket platform," International Journal of Scientific & Engineering Research, 2017.
- [8] Longuet-Higgins, M. S. "On the joint distribution of wave periods and amplitudes in a random

- wave field," in Proceeding of The Royal Society, 1983.
- [9] Goda, Y. in random seas and design an maritime structures, 2000, p. 42.
- [10] Center, N. D. B. "Nondirectional and directional wave data analysis procedures," 2003.
- [11] Institute, A. P. "Recommended practice for planning, designing, and constructing fixed offshore platforms—Working stress design," 2014.
- [12] Pei, X., Cao, Y., Gu, T., Xie, M., Dong, P., Wei, Z., Mei, J. and Zhang, T. "Generalizing multiaxial vibration fatigue criteria in the frequency domain: A data-driven approach," International Journal of Fatigue, 2024. https://doi.org/10.1016/j.ijfatigue.2024.108390
- [13] Fan, W., Li, Z. and Yang, X. "A spectral method for fatigue analysis based on nonlinear damage model," International Journal of Fatigue, 2024.https://doi.org/10.1016/j.ijfatigue.2024.10 8188
- [14] Xu, S., Rezanejad, K., Gadelho, J. and Soares, C. G. "Influence of the power take-off damping of a dual chamber floating oscillating water column on the mooring fatigue damage," Ocean Engineering, 2022. https://doi.org/10.1016/j.oceaneng.2022.1108
- [15] Hasselmann, K., Barnett, T., Bouws, E., Carlson, H., Cartwright, D., Enke, K., Ewing, J., Gienapp, H., Hasselmann, D. and Kruseman, P. "Measurements of wind-wave growth and swell decay during the Joint North Sea Wave Project (JONSWAP)," Deut. Hydrogr. Z.. , 1973.
- [16] Thompson, I. "Validation of naval vessel spectral fatigue analysis using full-scale measurements,"

 Marine Structures, 2016.

 https://doi.org/10.1016/j.marstruc.2016.05.00
- [17] Magoga, T. "Fatigue damage sensitivity analysis of a naval high speed light craft via spectral fatigue analysis," Ships and Offshore Structures, 2019.
 - https://doi.org/10.1080/17445302.2019.161254
- [18] Xu, S. and Soares, C. G. "Evaluation of spectral methods for long term fatigue damage analysis of synthetic fibre mooring ropes based on experimental data," Ocean Engineering, 2021. https://doi.org/10.1016/j.oceaneng.2021.108842

Copyright [©] Int. J. of GEOMATE All rights reserved, including making copies, unless permission is obtained from the copyright proprietors.